Article

Integration of Hydrothermal Carbonisation and Anaerobic Digestion for the Energy Valorisation of Grass

Aaron E. Brown [1], James M. Hammerton [1], Miller Alonso Camargo-Valero [2,3] and Andrew B. Ross [1,*]

1 School of Chemical and Process Engineering, University of Leeds, Leeds LS2 9JT, UK;
a.e.brown@leeds.ac.uk (A.E.B.); j.m.hammerton@leeds.ac.uk (J.M.H.)

2 BioResource Systems Research Group, School of Civil Engineering, University of Leeds, Leeds LS2 9JT, UK;
m.a.camargo-valero@leeds.ac.uk

3 Departamento de Ingeniería Química, Campus La Nubia, Universidad Nacional de Colombia,
Manizales 170002, Colombia

* Correspondence: a.b.ross@leeds.ac.uk; Tel.: +44-(0)113-343-1017

Abstract: The integration of hydrothermal carbonisation (HTC) and anaerobic digestion (AD) can overcome some of the disadvantages of thermal or biological processing alone. This study aims to investigate integrated HTC-AD across a range of integration strategies and HTC processing temperatures (150 °C, 200 °C and 250 °C) to improve the energy conversion efficiency (ECE) of grass, compared to AD alone. The separation of hydrochars (HCs) for combustion and process waters (PWs) for digestion appears to be the most energetically feasible HTC-AD integration strategy, compared to HC or HTC-slurry AD. Hydrochars represent the greater energy carrier with between 81–85% of total energy output. The ECE of grass was improved from 51% to 97% (150 °C), 83% (200 °C) and 68% (250 °C) through integrated HTC-AD. Therefore, lower HTC processing temperatures yield more favourable energetics. However, higher HTC temperatures favour more desirable HC properties as a combustion fuel. The hydrochar produced at 250 °C (HC-250) displayed the highest HHV (25.8 MJ/kg) and fixed carbon: volatile matter ratio (0.47), as well as the greatest reduction in slagging and fouling potential (ash flow temperature > 1550 °C). Overall, integrated HTC-AD is an effective energy valorisation strategy for grass. A compromise exists between the quality of hydrochar and the energetic balance. However, at 250 °C the process remains energetically feasible (EROI = 2.63).

Keywords: grass; hydrothermal carbonisation; anaerobic digestion; integration; hydrochar; process water; biomethane; pre-treatment; affordable and clean energy

1. Introduction

Grass is a widely abundant, terrestrial lignocellulosic biomass which covers approximately 26% of the total global land area [1]. The term 'grass' encompasses a range of biomass types, from purpose-grown energy crops such as miscanthus [2] to a composite mixture of grass species such as those harvested from roadside verges [3]. Grasses are typically defined as monocotyledonous plants which are part of the *Poaceae* family [4]. Table 1 shows the typical biochemical compositions of different grass types (miscanthus, switchgrass, reed canary grass and marginal land grass) are largely varied.

The utilisation of grass as a feedstock to generate bioenergy is well established, with a particular interest regarding applications in biological conversion processes [5,6]. However, the recalcitrant lignocellulosic structure of grass means its biodegradability is typically limited during anaerobic digestion (AD), often requiring pre-treatment to improve biomethane yields [6]. Alternative biomass conversion routes are based on thermochemical methods, including combustion, pyrolysis and gasification [7]. However, the physiochemical properties of grasses mean that thermal processing can prove problematic. Such characteristics include a high moisture content, low bulk density and limited friability [2]. Furthermore,

an unfavourable ash composition, containing high concentrations of alkali metals and chlorine, means thermal conversion of grasses can lead to potential slagging, fouling and corrosion issues [2,8,9]. Table 1 shows that grass harvested from marginal land typically contains higher concentrations of problematic alkali metals and chlorine. However, utilisation of grass from marginal land could be advantageous over purpose-grown energy crops (e.g., miscanthus), as this reduces the competition for fertile land that could be used for alternative purposes, such as food-crop production or animal husbandry.

Table 1. Comparative biochemical composition of different grass sources.

Composition	Miscanthus	Switchgrass	Reed Canary Grass	Marginal Land Grass [b]
Cellulose (%db)	44–45	30–45	26–39	20–33
Hemicellulose (%db)	18–30	21–35	17–28	24
Lignin (%db)	14–22	7–23	4–5	10–25
Protein (%db)	NR	3–11	16	7–16
Ash (%db)	2–7	2–10	1–13	8–27
Alkali Metals [a] (%db)	0.1–1.0	0.2–1.3	0.2–3.8	0.4–4.4
Chlorine (%db)	0.0–0.6	0.0–0.5	0.0–0.6	0.1–2.0
Additional References	[2,8,10–12]	[12]	-	[3,13–16]

Data collated by combining information presented in the Phyllis2 database [17] with additional references, as specified. db = dry basis. NR = not reported by references. [a] Na and K content. [b] includes grass sourced from: riverbanks, road-verges, nature reserve, residential clippings, lawn cuttings and University campuses.

Hydrothermal carbonisation (HTC) is an alternative thermochemical process involving the conversion of biomass in hot compressed water, maintained under subcritical conditions [18]. Under these conditions, water becomes less polar, through the weakening of hydrogen bonds, to form reactive hydronium (H_3O^+) and hydroxide (OH^-) ions [19]. This reaction medium facilitates the conversion of biomass into three different products, hydrochars (solid phase), process water (aqueous phase) and gas (gaseous phase), through a number of complex and simultaneous reaction pathways [20]. As HTC is conducted in water, it benefits from the advantage of being able to process biomass with a high moisture content without the need for energy-intensive drying processes [19]. Hydrochars are carbonaceous, 'coal-like' solids with typically improved characteristics as solid combustion fuels, including increased Higher Heating Value (HHV) [2,8,10], reduced slagging and fouling potential due to the selective demineralisation of problematic inorganics [2,8,10,12] and improved friability [2]. The typical HHV of miscanthus is between 15.2–18.4 MJ/kg [2,8,10–12], whereas the HHV of miscanthus-derived hydrochars increases to between 17.9–24.5 MJ/kg and 24.8–32.1 MJ/kg following HTC at temperatures of 200 °C and 250 °C, respectively [2,8,10–12]. Higher processing temperatures generally yield hydrochars with higher HHV; however, this is also influenced by residence time [10]. As well as miscanthus, HTC has also been used to generate solid combustion fuel from switchgrass [12], energy grass [21], lawn grass [22] and grass from a University campus [15].

Traditionally, hydrochars are considered the product of interest from HTC. However, large quantities of process waters are also produced, which contain a complex mixture of solubilised organic and inorganic matter originating from the biomass [23,24]. The process water can contain 30–50% of the original carbon from the biomass [24]. However, this is dependent on feedstock selection and HTC reaction severity [23]. Therefore, energy valorisation of the process water via biological conversion alongside hydrochar can potentially improve the overall energy recovery efficiency of the process.

There appears to be an ever-increasing interest in the integration of HTC and AD (HTC-AD) in order to fully maximise the energetic potential of biomass. A number of HTC-AD integration strategies exist, including the combustion of hydrochar and AD of the process water [25–30], AD of hydrochars [25,26,31] or AD of slurries (mixed hydrochars and process water) following hydrothermal pre-treatment [25,26,29,30,32,33]. Generally, the separation of hydrochars for combustion and process waters for digestion is the most

energetically feasible conversion route [25,26,29,30]. However, the slagging and fouling behaviour of some hydrochars, such as those produced from water hyacinth [26] and digestates [34] remains problematic, limiting their potential application in large-scale combustion facilities. Therefore, the approach for integrating HTC-AD is likely to depend upon integration strategy selection, reaction severity, feedstock selection, properties of the hydrothermal products and downstream applications of products.

The integration of HTC-AD using lignocellulosic biomass is only sparsely reported across literature studies. The potential for biomethane generation from lignocellulosic-derived HTC process waters was investigated by Pagés-Díaz et al. [35], comparing four types of biomass processed at 220 °C for 60 min. Biomethane yields were found to vary considerably between the different biomasses as a result of differing N contents and the resultant formation of nitro-recalcitrant compounds. However, the effect of reaction severity was not explored. Recently, Parmar et al. [36] demonstrated that HTC reaction temperature influences the biomethane yields subsequently generated by lignocellulosic-derived HTC process waters produced from grass, privet hedge clippings and woodchips. Higher biomethane yields were observed for process waters produced at intermediate HTC temperatures (200 °C), compared to lower (150 °C) or higher temperatures (250 °C).

Limited studies exist comparing different HTC-AD integration strategies using lignocellulosic biomass as a feedstock. Wang et al. [15] investigated an alternative HTC-AD integration strategy by comparing the properties of hydrochar produced from grass and grass-derived digestates, following biomethane potential (BMP) experiments conducted for 7- and 14-day durations. Hydrochars produced from grass-digestate displayed increased hydrochar yields and HHVs, compared to hydrochars produced from untreated grass. The combined energy obtained from biogas and hydrochar production improved the energy conversion efficiency (ECE) of grass to 66.5% and 71.3% after 7- and 14-day digestions, respectively, compared to the ECE of untreated grass hydrochar alone (63.9%). Brown et al. [26] compared the improvement in energy recovery from water hyacinth, using a range of HTC-AD integration strategies and process temperatures. Separating hydrochars for combustion and process waters for AD was found to provide the greatest energy recovery compared to AD alone, with lower processing temperatures providing more favourable energetics. However, the hydrochars displayed potential slagging and fouling issues, limiting their application in combustion, particularly at larger scales. As a result, hydrothermal pre-treatment at the lowest reaction severity (150 °C, 60-min) and AD of the slurry was identified as a feasible HTC-AD strategy, and improved the anaerobic biodegradability of the water hyacinth from 30% to 58%.

The aim of this study is to investigate the integration of HTC-AD to improve the ECE of grass compared to AD alone. This included a comparison of three HTC-AD integration options: (i) hydrochar combustion and process water AD, (ii) AD of hydrochars alone and (iii) AD of HTC slurries, each across three HTC reaction severities: (a) 150 °C, 60 min, (b) 200 °C, 60 min and (c) 250 °C, 60 min. The novelty of this work explores the behaviour of grass during integrated HTC-AD, for the first time, across a range of integration strategies and HTC reaction severities. The research provided a greater understanding of the application of hydrothermal carbonisation of lignocellulosic biomass integrated with anaerobic digestion.

2. Materials and Methods

2.1. Sample Collection and Preparation

2.1.1. Grass

Grass clippings were collected from the University of Leeds campus, UK (53°48′25.9″ N 1°33′18.8″ W), in August 2018 and oven dried at 60 °C (Memmert, Büchenbach, Germany) for a minimum of 24 h. The particle size was reduced to <1 mm using a domestic blender (NutriBullet) for use in subsequent HTC reactions and biochemical methane potential (^{E}BMP) tests. The particle size of grass and hydrochars were reduced to <100 μm using a Cryomill (Retsch, Haan, Germany) to determine proximate, ultimate and inorganic composition.

2.1.2. Inoculum

Inoculum used for biochemical methane potential (^{E}BMP) experiments was collected from an AD reactor processing sewage sludge at Yorkshire Water's Esholt Wastewater Treatment Plant (WWTP), West Yorkshire, UK. The inoculum was homogenised using a 1 mm sieve to remove large particles and stored at 4 °C until required (<1 month). Before starting the biochemical methane potential experiments, the inoculum was incubated at 37 °C using a water bath for approximately 48 h to reduce enteric methane emissions during the experiments.

2.2. Hydrothermal Carbonisation (HTC) Reactions

2.2.1. HTC Reaction Conditions

HTC reactions were carried out in triplicate using a bench-top Parr (Parr, Moline, IL, USA) 600 mL non-stirred reactor, using a quartz glass reactor liner. Reactions were conducted according to the same methodology reported by Brown et al. [25]. In short, a 20 g subsample of oven dried grass was mixed with 200 mL of distilled water to create an approximate solid loading ratio (SLR) of 10%. Reactions were conducted at 150 °C, 200 °C and 250 °C, corresponding to pressures of approximately 4 bar, 14 bar and 43 bar, respectively. The Parr reactor was heated using an electrical heating jacket, controlled by a proportional integral derivative (PID) controller. The heating rate of the reactor was approximately 8 °C/min. Following a 60 min retention time, the reactor was removed from the heating jacket and allowed to cool to ambient temperature in a vented fume hood.

2.2.2. HTC Mass Balance

Once cooled, the gas was vented from the reactor and the solid and aqueous fractions separated through Büchner filtration using Whatman Grade 4 filter paper. The residual solid (hydrochar) was dried overnight (60 °C) before weighing. Hydrochar yield (HY) was determined using Equation (1), depending on the mass of residual hydrochar (g) and mass of grass (g) added to the HTC reactor. Gaseous yield was determined through the percentage difference between total inputs and output of the HTC reaction. Process water yield was determined by the difference. The hydrothermal products of similar HTC reaction conditions were combined and homogenised to ensure enough material for subsequent characterisation and conversion.

$$\text{HY (\%)} = \frac{\text{Mass of Hydrochar}}{\text{Mass of Grass}} \times 100 \tag{1}$$

Herein, hydrochars (HC), process waters (PW) and HTC slurries are referred to as 'HC-150, HC-200, HC-250', 'PW-150, PW-200, PW-250' and 'Slurry-150, Slurry-200 and Slurry-250', respectively, depending on the HTC processing temperature.

2.2.3. Hydrothermal Severity Factor

The severity factor (SF) of HTC reactions were described according to Equation (2) [37], where *t* represents reaction retention time (min) and *T* represents reaction temperature (°C).

$$\text{SF} = \log\left[\, t \times \exp\left(\frac{T - 100}{14.75}\right)\right] \tag{2}$$

2.3. Biochemical Methane Potential

2.3.1. Theoretical Biochemical Methane Potential

The theoretical biochemical methane potential (^{T}BMP) values of untreated grass, hydrochars and HTC slurries were calculated according to Boyle's equation (Equation (3)) [30]. Here, c, h, o and n represent the molar fractions of C, H, O and N, respectively. It was assumed that the untreated grass and HTC slurries had the same elemental composition, due to difficulties in measuring the elemental composition of aqueous samples. The ^{T}BMP

of process waters was determined based on the theory that 1 g COD generates 350 NmL CH_4 under STP (1 atm, 0 °C and zero moisture content) [38].

$$\text{Theoretical BMP} = \frac{22,400\left(\frac{c}{2} + \frac{h}{8} - \frac{o}{4} - \frac{3n}{8}\right)}{12c + h + 16o + 14n} \tag{3}$$

2.3.2. Experimental Biochemical Methane Potential

The experimental biochemical methane potential (^{E}BMP) values of the grass and HTC products were determined using an AMPTS II (Bioprocess Control, Lund, Sweden), according to Brown et al. [26]. ^{E}BMP reactors were incubated for 30 days; by this point methane production was <1% of the total cumulative methane production throughout three consecutive days across all samples. Measured biomethane volumes were automatically normalised to STP (1 atm, 0 °C and zero moisture content) using the AMPTS II. The biodegradability (BI) of samples was calculated according to Equation (4), adapted from Wall et al. [5].

$$\text{BI (\%)} = \frac{E_{BMP}}{T_{BMP}} \times 100 \tag{4}$$

2.4. Analytical Methods

2.4.1. Solid Sample Analysis

Proximate analysis was determined by thermogravimetric analysis using a TGA/DSC 1 (Mettler Toledo, Columbus, OH, USA). Approximately 10 mg of sample was heated under nitrogen from 25 °C to 105 °C at a rate of 25 °C/min and held for 10 min. The sample was further heated under nitrogen from 105 °C to 900 °C at a rate of 25 °C/min. Once a temperature of 900 °C was achieved the sample was held for 10 min under nitrogen, then subsequently under air for 15 min. Ultimate (CHNS) composition was determined using a Flash 2000 CHNS analyser (Thermo Scientific, Waltham, MA, USA), which was calibrated using certified reference materials (Elemental Microanalysis, Okehampton, UK). Hydrogen content was corrected for moisture content and oxygen content was determined by difference. The biochemical composition (cellulose, hemicellulose and lignin) was calculated from the neutral detergent fibre (NDF), acid detergent fibre (ADF) and acid detergent lignin (ADL), determined using the Gerhardt Fibrecap system. Total solids (TS) and volatile solids (VS) were calculated gravimetrically by drying at 105 °C and subsequently ashing at 550 °C for 2 h [39]. The VS content of HTC slurries was calculated based on separate hydrochar and process water VS analysis before recombining these products according to the HTC yields, described in Section 2.2.2. Higher heating values (HHVs) were measured using a Parr 6200 bomb calorimeter (Parr, Moline, IL, USA), according to BS ISO 1928:2009 and predicted using Dulong's equation, shown in Equation (5) [26]. The energy densification (ED) and energy yield (EY) of the hydrochars were calculated according to Equations (6) and (7), respectively, using HHV data obtained from bomb calorimetry. Fuel burning profiles were determined by derivative thermogravimetric (DTG) analysis (TGA/DSC 1, Mettler Toledo, Columbus, OH, USA) by heating 10 mg of sample to 900 °C at 10 °C/min, as reported by Smith and Ross [10].

$$\text{HHV (MJ/kg)} = (0.3383 \times C(\%)) + \left(1.422 \times \left(H(\%) - \left(\frac{O(\%)}{8}\right)\right)\right) \tag{5}$$

$$\text{ED} = \frac{\text{HHV of Hydrochar}}{\text{HHV of Grass}} \tag{6}$$

$$\text{EY (\%)} = \text{ED} \times \text{HY} \tag{7}$$

Inorganic composition was determined using X-ray fluorescence (XRF) spectrophotometry (ZSX Primus II, Rigaku, Japan). Samples were prepared as pressed pellets. Briefly, 2.7 g of sample was mixed with 0.3 g CEREOX®® wax binder (FLUXANA®® GmbH & Co. KG,

Bedburg-Hau, Germany) using a vortex mixer (MU-K-MIXER_50Hz, FLUXANA®® GmbH & Co. KG, Bedburg-Hau, Germany). The mixed sample and binder were transferred to a 35 mm steel die and introduced to 10 t of pressure for approximately 5 min (Specac Press, Orpington, UK) to form a pressed pellet. Predicted slagging and fouling indices were calculated from the inorganic oxide composition of the samples. Further details regarding the calculation and interpretation of these indices are reported by Brown et al. [26]. Ash fusion testing was conducted using a Carbolite digital ash fusion furnace, according to DD CEN/TS 15370-1:2006.

2.4.2. Aqueous Sample Analysis

Chemical oxygen demand (COD), total phenols (TP), total nitrogen (TN) and ammonium–nitrogen (NH_4^+-N) concentrations were measured using HACH-lange cuvettes (Düsseldorf, Germany) LCK014, LCK346, LCK338 and LCK303, respectively. Total organic carbon (TOC) concentration was determined as the difference between total carbon (TC) and total inorganic carbon (TIC), measured using a HACH IL 500 TOC-TN analyser. The TS content of process water was determined gravimetrically by drying a known volume (c. 5 mL) at 60 °C, before subsequently ashing at 550 °C for 2 h to determine the VS content. A drying temperature of 60 °C was selected instead of 105 °C to reduce the losses of volatile components. The pH of the aqueous samples was measured using a digital pH meter (HQ11D, HACH, Ames, IA, USA). The composition of volatile fatty acids (VFAs) was determined according to Brown et al. [25]. Total VFA concentration was reported as the sum total of acetic, propionic, isobutyric, butyric, isovaleric, valeric, isocaproic, caproic, and heptanoic acid concentrations.

2.5. Energy Balance Calculations

The energy balance was calculated based on the energy input (EI) required to heat the HTC reactor compared against the energy output (EO) obtained from HHV of the conversion of the different HTC products. The energy balance was calculated based on a starting point of 1 kg of oven dried grass. The yields of hydrothermal products were extrapolated from the yield calculations described in Section 2.2.2.

The energy input was calculated based on Equation (8), adapted from [32]. Here, V_w is the volume of water added to the HTC reactor (L), C_w and C_b represent the specific heating capacities (MJ/kg/K) of water and biomass (grass), respectively, M_b is the mass of biomass (grass) added to the HTC reactor (kg), T_{reac} represents the final temperature of the HTC reaction (°C) and T_{amb} represents the assumed ambient temperature (25 °C). The assumed specific heating capacities of water and biomass (grass) were 4200 J/kg/K and 1455 J/kg/K, respectively [26]. In addition, 1 mL of water had an assumed mass of 1 g.

$$\text{Energy Input HTC (MJ/kg)} = \frac{(V_w C_w + M_b C_b) \times (T_{reac} - T_{amb})}{M_b} \tag{8}$$

The energy outputs obtained for the anaerobic digestion of untreated grass, hydrochars, process waters and slurries, as well as the energy output from hydrochar combustion, were calculated according to the methods reported by Brown et al. [26]. The HHVs used for calculating the energy output of hydrochar combustion were obtained via bomb calorimetry on an as-received basis.

Energy return on energy investment (EROI) was calculated according to Equation (9); assuming a 55% heat recovery efficiency [26]. The energy recovery efficiency (ECE) of each integration strategy was determined according to Equation (10). The HHV of the untreated grass used in ECE calculations was based off the value obtained from bomb calorimetry on an as-received basis.

$$\text{EROI} = \frac{\text{EO}}{(\text{EI} \times 0.45)} \tag{9}$$

$$\text{ECE (\%)} = \frac{\text{EO}\left(\frac{\text{MJ}}{\text{kg}}\right)}{\text{HHV of Grass}\left(\frac{\text{MJ}}{\text{kg}}\right)} \times 100 \tag{10}$$

2.6. Error and Statistical Analysis

HTC reactions were performed in triplicate. [E]BMP and analytical methods were performed in duplicate, with the exceptions of TGA, biochemical composition, bomb calorimetry and XRF analyses. Average values are reported alongside standard deviation values, with the exception of [E]BMP, where average values are presented alongside the maximum and minimum values. R^2 and line equations were calculated using Microsoft Excel. General linear model analysis was conducted using SPSS (version 25) with normal data distribution confirmed using Kolmogorov–Smirnov tests.

3. Results and Discussion

3.1. Influence of HTC on Hydrochar Properties

3.1.1. Proximate, Ultimate and Energy Densification Properties

Table 2 shows the proximate and ultimate analysis of the grass and hydrochars. Generally, a simultaneous reduction in volatile matter (VM) and increase in fixed carbon (FC) was observed with increasing HTC processing temperature. This behaviour is typically observed for lignocellulosic feedstocks [2,26]. HC-150 was the exception to this observation, displaying a slight increase in VM content compared to grass. The increase in VM between untreated grass and HC-150 is due to a reduction in the inorganic content of HC-150 (5.6%), compared to untreated grass (11.0%). A high VM content reduces the quality of a solid combustion fuel by causing flame instability and results in subsequent losses in heat, whereas a high FC content can increase combustion temperatures by producing a more stable flame [27]. The FC:VM, or fuel ratio, is used to rank the suitability of hydrochars as alternative, coal-like fuels [40]. Table 2 shows that HC-150 had a similar FC:VM to grass (0.21), whereas the FC:VM for HC-200 (0.30) and HC-250 (0.47) displayed an increase, indicating a more stable flame during combustion. However, the FC:VM of hydrochars remains significantly lower than coal (1.5) [41], as the VM content of hydrochars remains high.

Table 2. Proximate and ultimate composition of grass and hydrochars.

Analysis	Grass	HC-150	HC-200	HC-250
VM (%db)	73.8	77.7	69.7	58.6
FC (%db)	15.2	16.6	20.7	27.4
Ash (%db)	11.0	5.6	9.6	14.0
C (%db)	44.2 ± 1.0	45.2 ± 0.4	49.0 ± 0.6	57.2 ± 0.2
H (%db)	6.9 ± 0.8	6.1 ± 0.2	6.3 ± 0.4	6.1 ± 0.2
N (%db)	3.9 ± 0.1	3.0 ± 0.1	3.0 ± 0.0	3.4 ± 0.0
S (%db)	ND	0.4 ± 0.0	0.4 ± 0.0	0.4 ± 0.0
O [a] (%db)	34.0 ± 1.7	39.7 ± 0.3	31.8 ± 0.2	18.9 ± 0.1
FC:VM	0.21	0.21	0.30	0.47
H:C [b]	1.88	1.62	1.53	1.28
O:C [b]	0.58	0.66	0.49	0.25
C:N [c]	11.3	15.1	16.3	16.8
TS (%ar)	95.4 ± 0.9	93.8 ± 0.1	95.6 ± 0.0	97.5 ± 0.1
VS (%ar)	84.3 ± 0.7	83.0 ± 0.1	84.0 ± 0.2	81.5 ± 0.0
VS (%TS)	88.3	88.5	87.9	83.6
HHV [d] (MJ/kg db)	18.8	16.9	19.8	24.7
HHV [e] (MJ/kg db)	18.2	19.9	22.0	25.8

[a] Oxygen measured by difference. [b] Molar ratio. [c] Mass ratio. [d] HHV calculated using Dulong's equation. [e] HHV determined by bomb calorimetry. db = dry basis. ar = as received basis. VM = volatile matter. FC = fixed carbon. TS = total solids. VS = volatile solids. HHV = higher heating value. ND = not detected. Data are reported at average values ± one standard deviation, where applicable.

The ash content of grass was 11.0%; typically, lower values are observed in miscanthus (2–5%) [2,8,10,12]. The ash content of grass is highly varied across literature studies, but tends to appear higher in grasses collected from marginal land, such as riversides (9%) [42], sports fields (14.5%) [9] roadsides (17.9%) [3], University campuses (21.1%) [14] and residential areas (27.2%) [16]. HC-150 and HC-200 showed a reduced ash content compared to grass; however, the ash content of HC-250 (14.0%) was higher than grass. The cellulose (24.9% db) and hemicellulose (24.2% db) contents of grass were in agreement with the data presented for marginal land grasses in Table 1; however, the lignin content (3.8% db) was slightly lower.

The C content of hydrochars increased with increasing HTC temperature, to a maximum of 57.2% (HC-250). All hydrochars displayed a greater C content compared to grass. The O contents of the higher temperature hydrochars (HC-200 = 31.8% and HC-250 = 18.9%) were lower than grass (34.0%), reflecting a reduction in O content at higher HTC processing temperatures. The O content of HC-150 (39.7%) was higher than grass. Generally, increased HTC temperatures result in a simultaneous increase in the C content and reduction in O content when processing lignocellulosic biomass [8,21]. As a result, the O:C and H:C ratios tend to decrease at higher temperatures, due to the removal of carboxyl (–COOH) and carbonyl (C=O) groups via decarboxylation reactions and the removal of hydroxyl groups (–OH) via dehydration reactions during the HTC process [8,27]. This is reflected in Table 2, where HC-200 and HC-250 displayed reduced O:C and H:C compared to grass. However, HC-150 showed increased O:C compared to grass, indicating limited energy densification.

A high N content or S content is potentially problematic for the application of biomass or hydrochar as a combustion fuel due to the release of NO_x and SO_x emissions, resulting in severe human health and environmental impacts [43]. All hydrochars showed reduced N contents compared to grass, although N contents remained high ($\geq$3.0%). Furthermore, the N content increased between HC-200 (3.0%) and HC-250 (3.4%), suggesting that high levels of nitrogen could remain problematic. In addition, all hydrochars shown in Table 2 had higher S contents compared to grass. Despite this, recent evidence suggests that lignocellulosic-derived hydrochars display lower NO_x and SO_2 emissions compared to the untreated parent feedstock, in this case water hyacinth [44]. However, the release of NO_x and SO_x emissions from hydrochars is likely to vary between feedstocks, with further research required to understand the potential implications of these emissions during combustion.

The HHVs of grass and hydrochars are presented as two values in Table 2: theoretically calculated using Dulong's equation and directly measured using bomb calorimetry. Calculated theoretically, the HHVs of HC-200 and HC-250 were both greater than grass, whilst HC-150 showed the lowest HHV due to its higher O content. Alternatively, a linear increase in HHV with increasing HTC temperature was observed whilst measuring HHV via bomb calorimetry. Despite containing the highest ash content, HC-250 showed the highest HHV, 25.8 MJ/kg, related to the lowest O:C ratio. Bomb calorimetry directly measures the gross heating value of a sample and can therefore be considered a more accurate measurement of HHV compared to predictive methods. Accordingly, the HHV values determined by bomb calorimetry were applied to all further calculations henceforth.

Figure 1 shows that the energy densification (ED) of hydrochars increased as HTC temperature increased. The EDs of HC-200 and HC-250 were 1.21 and 1.42, respectively. However, only limited ED was observed for HC-150 (1.09). By contrast, hydrochar yield (HY) showed an inverse relationship to ED, decreasing at increased HTC temperatures: 73.4% (HC-150), 57.0% (HC-200) and 37.4% (HC-250). HTC gas yields increased as temperature increased, but remained a small contribution to the overall mass balance (< 2%). The energy yield (EY) recovered by the hydrochars decreased with increasing HTC temperature, despite the greater ED: 80.2% (HC-150), 68.9% (HC-200) and 52.9% (HC-250), as a result of the decreased HY at higher temperatures. The lower EYs of hydrochars, particularly at higher processing temperatures, suggest that energy valorisation of the process water fraction could maximise the energy recovery efficiency of the process.
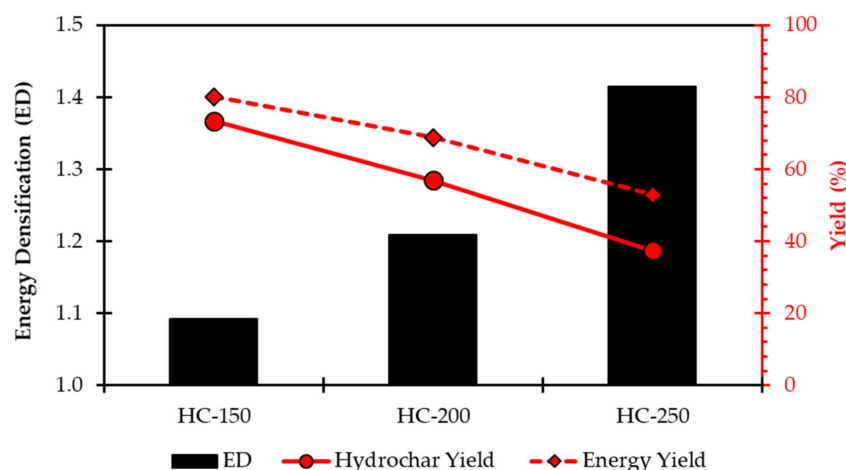
Figure 1. Energy densification, hydrochar yield and energy yield of hydrochars.

The limited ED and high HY of HC-150 could be a result of reduced hydrolysis reactions. Hydrolysis is the initial reaction mechanism of HTC, where complex organic polymers are broken down into their corresponding monomeric or oligomeric constituents, for example, the cleavage of the ester or ether bonds of cellulose or hemicellulose into monosaccharides or oligosaccharides [45]. The products of hydrolysis undergo subsequent reactions: dehydration, decarboxylation, condensation, polymerisation and aromatisation [20]. Hydrolysis of hemicellulose starts at approximately 180 °C and cellulose at approximately 230 °C [45]. Therefore, the limited ED and high HY of HC-150 could be a result of insufficient hydrolysis of the holocellulose fraction of grass at 150 °C.

The yields and properties of hydrochars vary depending on different HTC reaction conditions, with temperature generally regarded as the most influential parameter. However, additional factors, such as retention time, also influence hydrochar characteristics [10,46]. Variations in reaction conditions can create difficulties in cross-comparing data across multiple published studies. In an attempt to overcome this, HTC reaction temperature and retention time can be combined into a single factor, termed the 'severity factor' (SF) [37]. The SFs of the HTC reactions used during this study were 3.3 (150 °C), 4.7 (200 °C) and 6.2 (250 °C).

Figure 2 displays correlations between HTC SF and HY, HHV, ED and EY obtained from grass hydrochars, using a combination of data from literature studies [2,8,10–12,15,21,22] and this work. HHV values were corrected to a dry basis (db) where appropriate. Data points where the retention time was 0 min included in [10,21] were excluded from Figure 2, as this results in a SF of 0. HHV, ED and EY values reported for lawn grass by Guo et al. [22] were also excluded from Figure 2, as these data were not easily interpreted from the Figures presented in [22].

General linear model analysis confirmed a significant negative correlation between both HTC SF and HY ($p < 0.001$) (Figure 2a) and HTC SF and EY ($p < 0.01$) (Figure 2d). In addition, a significant positive correlation ($p < 0.001$) was identified between both HTC SF and HHV (Figure 2b) and HTC SF and ED (Figure 2c). However, the R^2 values show that the strength of correlation varied for each parameter, with HTC SF displaying correlations with HHV > HY > ED > EY ordered by strength. The correlations presented in Figure 2 do not account for variations in the behaviour of different grass species during HTC, or the effect of seasonal variation, which may introduce variability in hydrochar characteristics [2]. However, Figure 2 shows that the HY, HHV, ED and EY values generated by this study are in agreement with previous literature investigating the properties of grass-derived hydrochar.

Figure 3 shows the combustion profiles for the grass and hydrochars determined by DTG. HC-250 displays a different combustion profile compared to grass, HC-150 and HC-200, demonstrating a reduced mass loss at approximately 300 °C and a greater mass loss peak at approximately 450 °C. The reduced mass loss at approximately 300 °C is

indicative of the removal of cellulose from HC-250 [2], whilst the greater mass loss peak near 450 °C is characteristic of increased FC content [47], as shown in Table 2. The mass loss peak at 450 °C is reduced for grass, HC-150 and HC-200, compared to HC-250, whereas grass, HC-150 and HC-200 display a greater mass loss at approximately 400 °C, indicating a shift in combustion behaviour potentially linked to the increased aromatisation of furanic carbon in HC-250 [31]. The DTG analysis presented in Figure 3 suggests a more 'coal-like' combustion profile for HC-250 compared to grass, HC-150 and HC-200. This supports the findings of Smith et al. [2], who found that HCs produced from miscanthus at 250 °C displayed more 'coal-like' combustion properties compared to HCs produced at 200 °C.
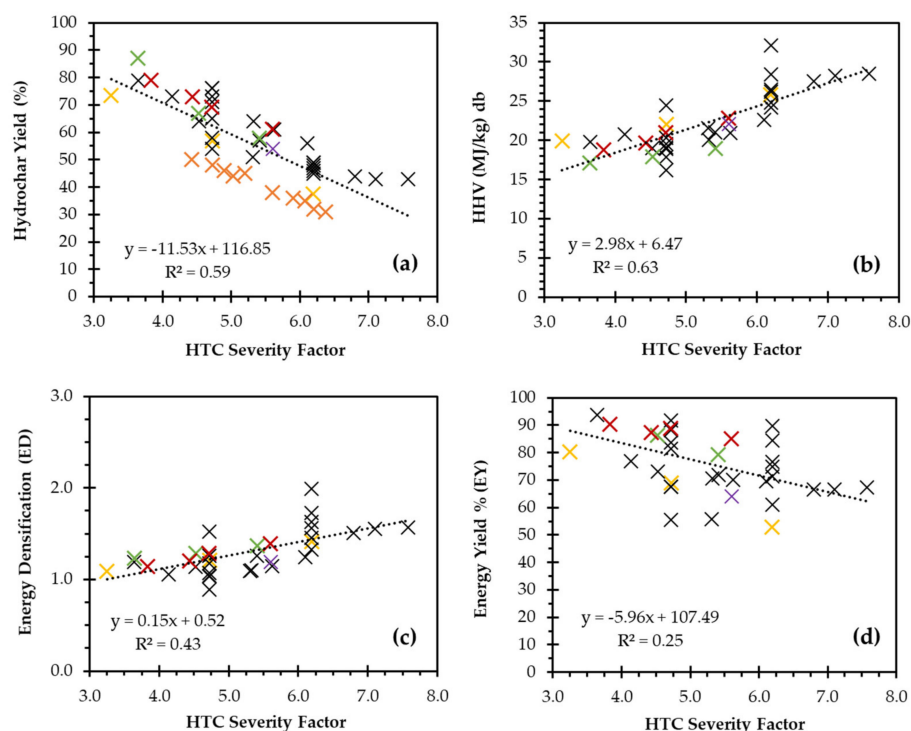
Figure 2. Correlations of HTC severity factor and hydrochar: (**a**) yield, (**b**) HHV, (**c**) energy densification, and (**d**) energy yield of grass-derived hydrochars. The different colours represent different grass types; black = miscanthus [2,8,10–12], green = switchgrass [12], red = energy grass [21], orange = lawn grass [22], purple = campus grass [15] and yellow = campus grass (this study).
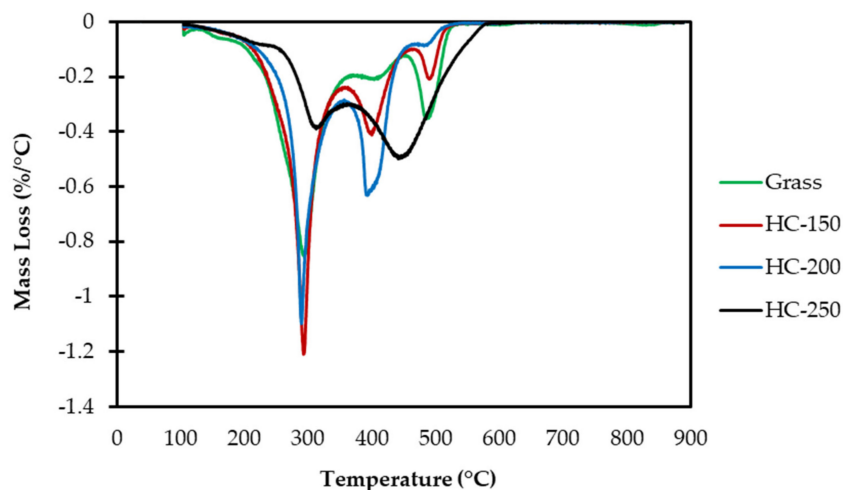
Figure 3. Derivative thermogravimetric (DTG) burning profiles of grass and hydrochars. Data is reported on a dry-ash-free basis.

3.1.2. Inorganic Composition and Behaviour of Ash during Combustion

The ash composition of a fuel is of vital importance to its application in large-scale combustion. High concentrations of alkali metals and chlorine can lead to unfavourable ash chemistry, resulting in issues such as slagging, fouling and corrosion [8,10]. Alkali metals generally reduce the melting temperature of ash, increasing the risk of slagging, whilst alkaline earth metals such as Ca and Mg generally increase the ash melting temperature, reducing the risk of slagging [8]. Fouling is caused when volatilised Na, K and Cl deposit onto cool surfaces [8].

Table 3 displays the major inorganic composition of the grass and hydrochars, as well as the removal efficiency of each element from the hydrochars, compared to grass. The major inorganic components of grass were K > Si > Ca > Cl > P. During HTC, biomass undergoes selective demineralisation of problematic inorganics, which become solubilised into the process water [8]. Table 3 shows increased removal efficiency for alkali metals (Na and K) and Cl (52–93%) compared to earth metals such as Ca (22–33%) and Mg (45–59%), agreeing with the findings of previous reports [8]. Furthermore, hydrochars produced at higher temperatures showed higher removal efficiency compared to hydrochars produced at lower temperatures. At 250 °C, 87–93% of the problematic Na, K and Cl had been removed from the solid fraction. Smith et al. [8] also reported more efficient Na and K removal from miscanthus during HTC at 250 °C (79–88%) compared to 200 °C (71–74%). The removal efficiencies of P and Ca decreased between HC-200 and HC-250, suggesting re-incorporation of these inorganics back into the hydrochars under more severe reaction conditions. Hydrochars produced at higher processing temperatures are thought to show increased surface functionality, which could facilitate the re-adsorption of inorganics in the process water [8].

Table 3. Inorganic composition of grass and hydrochars, alongside the removal efficiencies of inorganic species from hydrochars, compared to the original biomass.

Element	Grass	HC-150	HC-200	HC-250
Inorganic Content (wt% db)				
Na	0.1	0.0	0.0	0.0
Mg	0.3	0.2	0.2	0.4
Si	1.9	2.4	2.6	3.9
P	0.6	0.6	0.7	1.5
Cl	1.2	0.8	0.7	0.2
K	2.7	1.8	1.6	0.6
Ca	1.5	1.6	1.7	2.9
Fe	0.0	0.0	0.1	0.1
Removal Efficiency of Inorganics, Compared to Untreated Grass (%)				
Na	-	52	68	87
Mg	-	45	59	56
Si	-	7	22	24
P	-	21	33	1
Cl	-	55	68	93
K	-	53	67	92
Ca	-	22	33	25
Fe	-	13	15	14

db = dry basis.

Selective demineralisation of hydrochars during HTC has the potential to upgrade biomass to generate a solid fuel with improved combustion properties. Table 4 displays the predicted slagging and fouling behaviour of the grass and hydrochars based upon calculated indices. Grass is predicted to have medium or high slagging and fouling potential, likely related to high concentrations of K. HC-150 and HC-200 showed slight improvements in predicted slagging behaviour compared to grass, with the slagging index (SI) indicating low slagging potential and the slag viscosity index (SVI) indicating medium

slagging potential. However, all other indices suggested similar slagging and fouling issues to grass. By comparison, HC-250 displayed the greatest improvement in predicted slagging behaviour, showing improvement in the alkali index (AI), bed agglomeration index and fouling index (FI) compared to grass, HC-150 or HC-250. In addition, the SI and SVI suggest reduced slagging potential compared to grass. Therefore, according to Table 4, the hydrochar produced at the highest temperature showed the greatest reduction in predicted slagging and fouling propensity. This is linked to higher removal efficiencies of problematic alkali metals at higher HTC processing temperatures, as shown in Table 3.

Table 4. Predicted slagging and fouling indices for grass and hydrochars.

Sample	Slagging and Fouling Index					
	AI	BAI	Rb/a	SI	FI	SVI
Grass	1.84	0.02	1.4	0.6	4.8	61.3
HC-150	1.09	0.03	0.9	0.3	2.0	66.4
HC-200	0.89	0.04	0.8	0.3	1.6	66.5
HC-250	0.27	0.17	0.7	0.3	0.5	63.4

■ = low slagging/fouling potential. ■ = medium slagging/fouling potential. ■ = high slagging/fouling potential. AI = alkali index. BAI = bed agglomeration index. Rb/a = acid base ratio. SI = slagging index. FI = fouling index. SVI = slag viscosity index.

The slagging and fouling indices presented in Table 4 were initially developed to analyse coal samples with alumina–silicate ash compositions [8,12]. Therefore, these results must be interpreted cautiously when analysing biomass, as it is assumed that the biomass ash matrix behaves similarly to coal ash during combustion. Figure 4 displays the results of ash fusion tests for the grass and hydrochar ashes. Ash fusion tests provide a greater understanding of slagging behaviour by identifying the temperatures at which ashes undergo different formational changes. Transitional changes occurring at higher temperatures are indicative of reduced slagging potential [8].
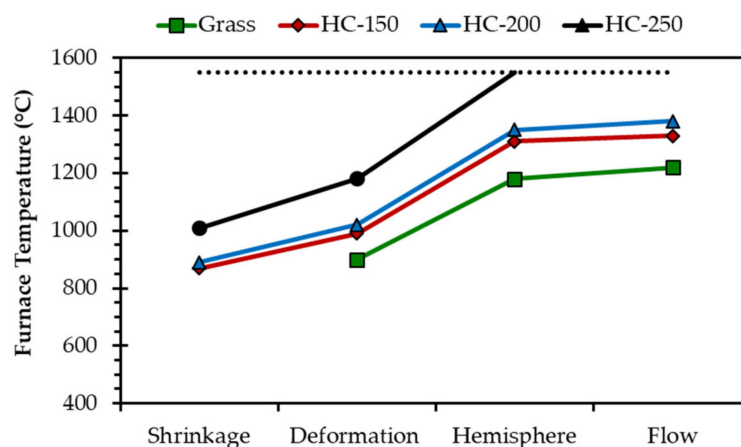
Figure 4. Ash fusion transition temperatures for grass and hydrochars. The dotted line indicates the temperature limit of the furnace (1550 °C).

According to Figure 4, both HC-150 and HC-200 displayed moderate reductions in slagging propensity compared to grass, whereas HC-250 showed the greatest reduction in slagging behaviour and therefore improvement in ash behaviour. The deformation, hemisphere and flow temperatures of the grass ash were 900 °C, 1180 °C and 1220 °C, respectively. The deformation temperature of the HC-250 ash was 1180 °C, whilst the hemisphere and flow temperatures were beyond the furnace limit (>1550 °C). Smith et al. [8] reported increased ash flow temperature for miscanthus-derived hydrochars produced at 200 °C (1550 °C) and 250 °C (>1570 °C) compared to untreated miscanthus (1350 °C), supporting the conclusions of Figure 4. The results of Figure 4 confirm the findings

of Table 4: that the hydrochars produced at the highest temperature (HC-250) showed the greatest reduction in slagging potential, due to the most efficient removal of alkali metals (Table 3). However, this effect is likely to be feedstock-dependent. HTC has been previously shown to increase the ash melting temperature of miscanthus and willow [8]. Whereas, Brown et al. [26] reported that the ash flow temperatures of untreated water hyacinth-derived hydrochars were lower than untreated water hyacinth, suggesting that HTC resulted in no significant improvement in ash behaviour.

Overall, hydrochar produced at 250 °C (HC-250) displayed more favourable combustion properties than grass and hydrochars produced at lower temperatures (HC-150 and HC-200). HC-250 showed the greatest FC:VM, HHV and ED, as well as the lowest slagging and fouling potentials: all desirable properties for a solid combustion fuel. However, the favourable combustion properties of HC-250 are compromised due to the lower HY, reducing the recovered EY, compared to hydrochars produced at a lower temperature.

3.2. Influence of HTC on Process Water Composition

The compositions of the HTC process waters (PW) are displayed in Table 5. The PW yields increased with increasing processing temperature, as intermediates from HTC reactions become increasingly solubilised into the aqueous phase. The concentrations of COD (33.0–34.6 g/L) and TOC (12.3–13.5 g/L) remained relatively constant across each HTC temperature. Total volatile fatty acid (VFA) concentrations increased at higher processing temperatures, a behaviour typically observed for lignocellulosic biomass [26,48,49]. Acetic acid represented the majority fraction (87–91%) of the total VFA concentration. Higher concentrations of VFA within PWs are beneficial for further conversion during anaerobic digestion, acting as a pre-cursor to methanogenesis.

Table 5. Composition of HTC process waters.

| Analysis	PW-150	PW-200	PW-250
PW Yield (%)	26.0 ± 2.8	42.2 ± 2.7	61.1 ± 4.0
COD (g/L)	34.6 ± 1.3	33.0 ± 0.6	34.2 ± 0.4
TOC (g/L)	13.5 ± 0.0	12.3 ± 0.0	12.4 ± 0.0
TS (g/L)	33.0 ± 0.1	27.1 ± 0.1	23.4 ± 0.0
VS (g/L)	27.2 ± 0.1	20.9 ± 0.0	18.2 ± 0.1
Ash (g/L) *	5.8 ± 0.1	6.5 ± 0.1	5.2 ± 0.1
Acetic Acid (mg/L)	721.1 ± 86.2	1529.0 ± 70.0	1911.2 ± 41.9
Propionic Acid (mg/L)	48.3 ± 16.9	81.0 ± 3.5	123.8 ± 7.1
Butyric Acid (mg/L)	33.6 ± 2.9	33.6 ± 17.4	45.2 ± 4.3
Total VFA (mg/L)	830.5 ± 73.5	1676.1 ± 47.3	2124.7 ± 57.4
Total Phenol (mg/L)	237.3 ± 8.8	345.8 ± 16.6	590.0 ± 28.3
TN (mg/L)	1236 ± 25	1520 ± 17	1482 ± 20
NH_4^+-N (mg/L)	224 ± 1	218 ± 6	260 ± 2
NH_4^+-N (%TN)	18	14	18
C:N	10.9	8.1	8.4
pH	4.6	4.1	4.7

* Calculated by difference. PW = process water. COD = chemical oxygen demand. TOC = total organic carbon. TS = total solids. VS = volatile solids. VFA = volatile fatty acid. TN = total nitrogen. C:N calculated as TOC (g/L)/TN (g/L). Data are reported at average values ± one standard deviation, where applicable.

The concentration of total nitrogen (TN) was higher for process waters produced at higher temperatures (PW-200 and PW-250) compared to PW-150, likely due to the increased degradation of proteins. PW-250 contained the highest concentration of NH_4^+-N, a known inhibitor of anaerobic digestion [50]. However, the proportional contribution of NH_4^+-N to TN remained similar among the PWs. Total phenol concentrations increased as HTC processing temperature increased, up to 590.0 mg/L (PW-250). This agrees with the findings of previous studies, which show an increase in the phenol concentrations of HTC process waters from lignocellulosic biomass at higher processing temperatures [26,48]. The phenol concentration of PW-250 was comparable to HTC process waters produced from corn stover

(413.8 mg/L) [48] and water hyacinth (424.8 mg/L) [26] at 250 °C. Phenols are derived from the lignin fraction of the grass and are also inhibitory to anaerobic digestion [51]. Each PW shown in Table 5 displayed an acidic pH (4.1–4.6), likely due to the solubilisation of VFAs.

3.3. Biomethane Potential of Hydrothermal Products

The experimental biomethane potential (^{E}BMP) curves from the untreated grass and HTC products—process waters, hydrochars and slurries—are presented in Figure 5, whereas the final ^{E}BMP, theoretical biomethane potential (^{T}BMP) and biodegradability (BI) results of grass and HTC products are presented in Table 6.
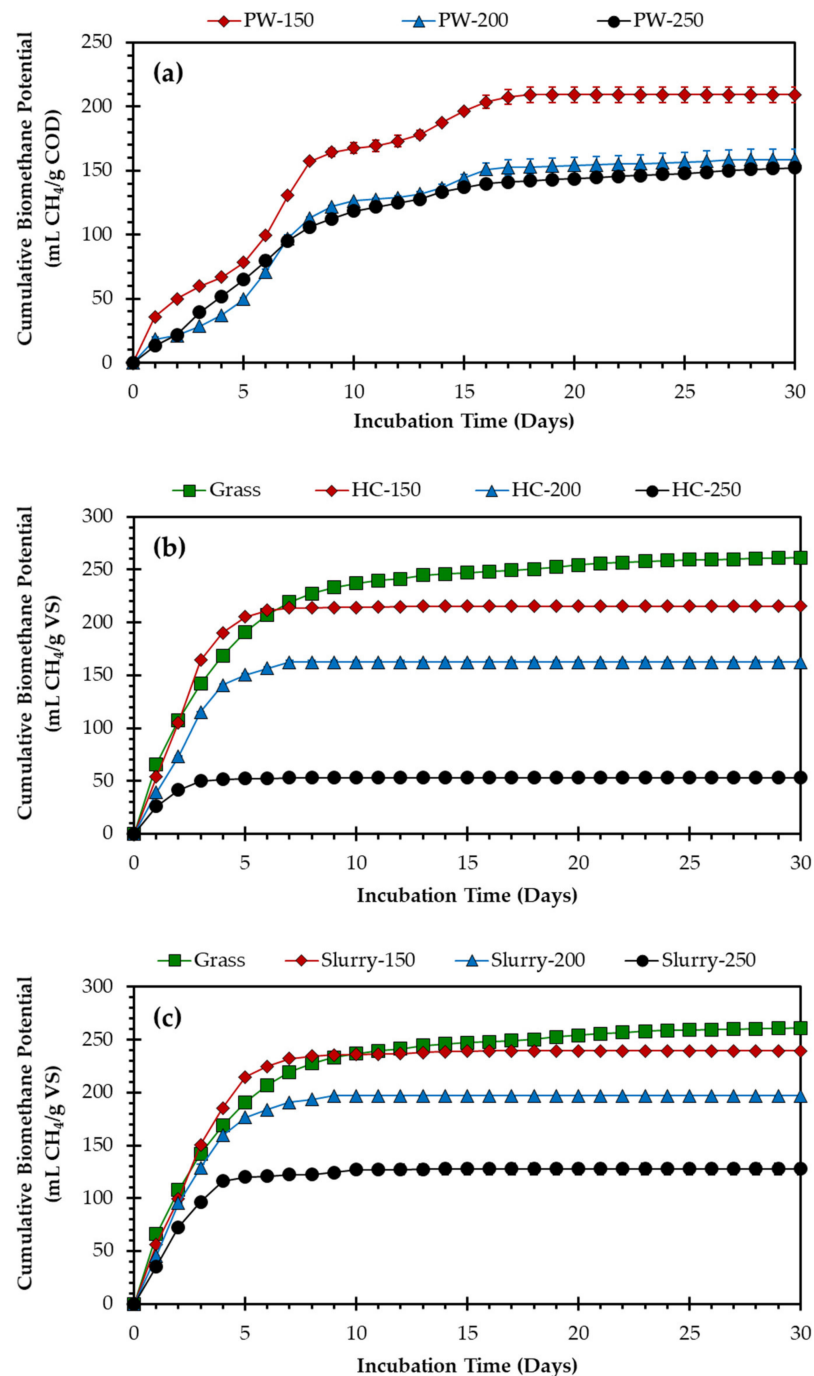
Figure 5. Experimental biomethane potential (^{E}BMP) of grass and HTC products: (**a**) process waters; (**b**) hydrochars; (**c**) slurries. Data are presented as average values. Error bars represent the maximum and minimum values (*n* = 2).

Table 6. Biodegradability index (BI) of grass and HTC products.

Sample	^{E}BMP (mL CH$_4$/g VS)	^{T}BMP (mL CH$_4$/g VS)	BI (%)
Grass	261.2	521.5	50
HC-150	215.4	463.3	46
HC-200	162.6	558.4	29
HC-250	53.2	721.7	7
Slurry-200	239.3	521.5	49
Slurry-200	196.9	521.5	38
Slurry-250	127.7	521.5	24
Sample	^{E}**BMP (mL CH$_4$/g COD)**	^{T}**BMP (mL CH$_4$/g COD)**	**BI (%)**
PW-150	209.3	350.0	60
PW-200	158.7	350.0	45
PW250	152.4	350.0	44

^{E}BMP = experimental biomethane potential. ^{T}BMP = theoretical biomethane potential. BI = biodegradability index.

3.3.1. Untreated Grass

Untreated grass had an ^{E}BMP of 261.2 mL CH$_4$/g VS as shown in Figure 5b,c. Previously reported biomethane potential values for grasses vary considerably: 222 mL CH$_4$/g VS [3], 261 mL CH$_4$/g VS [52], 285 mL CH$_4$/g VS [15], 292 mL CH$_4$/g VS [9], 308–340 mL CH$_4$/g VS [13], 327 mL CH$_4$/g VS [14], 341–493 mL CH$_4$/g VS [53], 400 mL CH$_4$/g VS [5] and 403 mL CH$_4$/g VS [16]. The variation in biomethane potential values is likely due to a combination of factors, including biochemical composition, plant maturity [6], interspecies variation [54], harvest season [13] and differences between the methodologies used to determine biomethane potential [53,55]. The ^{E}BMP results of the grass used in this study correspond with those previously reported for grass silage [52] and grasses collected from a University campus [15] and sports fields [9]. The ^{T}BMP of grass was 521.5 mL CH$_4$/g VS, corresponding to a BI of 50%. This suggests that the full energetic potential of grass was not achieved, and integrating HTC-AD has the potential to further improve the energy recovery of grass.

3.3.2. Process Waters

Figure 5a shows the ^{E}BMP of the PWs were 209.3 mL CH$_4$/g COD (PW-150), 158.7 mL CH$_4$/g COD (PW-200) and 152.4 mL CH$_4$/g COD (PW-250), corresponding to BIs of 60%, 45% and 44%, respectively (Table 6). Therefore, the PW produced at the lowest temperature (150 °C) yielded the highest ^{E}BMP: an increase of 32% and 37% compared to PW-200 and PW-250, respectively. The data presented in Figure 5a agrees with previous literature studies, which report PWs produced at lower temperatures generate a higher ^{E}BMP yield compared to PWs generated at higher temperatures. This trend has been identified for a range of biomass types, including cow manure [28], orange pomace [56], microalgae [27], macroalgae [25], water hyacinth [26] and the organic fraction from municipal solid waste [29]. Brown et al. [26] reported that the ^{E}BMP values of water hyacinth-derived PWs were 213.4 mL CH$_4$/g COD, 137.9 mL CH$_4$/g COD and 148.8 mL CH$_4$/g COD, using HTC processing temperatures of 150 °C, 200 °C and 250 °C, respectively. The values reported by Brown et al. [26] agree with the values presented in Figure 5a, indicating similar behaviour of lignocellulosic-derived PWs during AD. Conversely, Parmar et al. [36] reported that the biomethane yields of grass-derived HTC process waters were highest at intermediate HTC temperatures (200 °C), compared to less severe (150 °C) or more severe (250 °C) HTC conditions. Parmar et al. [36] conducted HTC reactions using a 20% SLR, whereas this study used a SLR of 10%, suggesting the composition of process waters and subsequent behaviour during AD could be affected by HTC SLR. Furthermore, Parmar et al. [36] used a 1:1 ISR during BMP experiments, whilst this study used a 2:1 ISR, which could influence digestion behaviour.

A recent review paper by Ipiales et al. [23] suggests that PWs produced below 200 °C perform better during AD due to the reduced prevalence of recalcitrant or inhibitory compounds solubilised within the PW. Table 5 shows that the concentration of total phenols was higher for the PWs produced at higher temperatures, suggesting that these would be inhibitory during AD [51]. Although not measured as part of this study, the concentration of readily digestible sugars is known to decrease at higher HTC temperatures [26,57], reducing the availability of accessible substrate for microbial metabolism. Furthermore, at temperatures of $\geq$200 °C, carbohydrate derivatives undergo dehydration reactions, forming HMF and furfural [48], which are also inhibitory to AD [51]. However, these recalcitrant compounds degrade further to organic acids under more severe HTC conditions. PW-250 contained the highest concentration of NH_4^+-N (Table 4), indicating an increased inhibitory potential of this PW. Recent studies highlighted the inhibitory potential of nitro-recalcitrant compounds [35] such as indoles [28]. More severe HTC conditions can increase the prevalence of inhibitory N-containing compounds in the process water through Maillard reactions between the carbohydrate and protein fractions [27,28]. Table 5 shows that TN concentration was higher for PWs produced at higher temperatures, potentially indicating the increased presence of inhibitory N-containing compounds. The C:N ratios of all process waters were below optimal for AD (25-30:1) [58], suggesting potential nitrogen inhibition. Overall, it appears that the PWs produced at higher temperatures contained the highest amounts of inhibitory material and were likely to contain reduced concentrations of carbon bioavailable for microbial metabolism, explaining the higher ^{E}BMP yield of PW-150 shown in Figure 5a.

3.3.3. Hydrochars

Figure 5b shows that the ^{E}BMP yields obtained from HCs were 215.4 mL CH_4/g VS, 162.6 mL CH_4/g VS and 53.2 mL CH_4/g VS for HC-150, HC-200 and HC-250, respectively, all lower yields than grass. It is widely reported that ^{E}BMP yield decreases as HC processing temperature increases [25,26,31]. Table 6 shows that despite ^{T}BMP increasing with increasing HTC processing temperature, BI was reduced at higher temperatures. This trend also reflects the findings of previous studies [26,31]. The BI of spent coffee-derived hydrochars reduced from 78% to 45% between 180 °C–250 °C [31], whilst the BI of water hyacinth-derived hydrochars reduced from 50% to 7% between 150 °C–250 °C [26], more closely reflecting the values presented in Table 6. Hydrochars produced at higher temperatures show an increased degree of aromatisation [31], creating a 'lignin-like' structure that undergoes more limited biodegradation [59]. The BI of HC-250 (7%) was particularly low (Table 6), demonstrating that the carbon availability for methanogenesis was limited for hydrochars produced at the highest temperature.

The results of Figure 5b and Table 6 indicate that the grass-derived hydrochars produced as part of this study are not a suitable feedstock for AD. Conversely, water hyacinth-derived hydrochars produced at 150 °C and 200 °C generated 85% and 80% higher ^{E}BMP yields compared to untreated water hyacinth [26]. This highlights differences in the behaviour of different types of lignocellulosic biomass during integrated HTC-AD.

3.3.4. HTC Slurries

Figure 5c shows that the ^{E}BMP yields of Slurry-150, Slurry-200 and Slurry-250 were 239.3 mL CH_4/g VS, 196.9 mL CH_4/g VS 127.7 mL CH_4/g VS, respectively, all lower than untreated grass. Lin et al. [60] found that hydrothermal treatment at 140 °C for 20 min (SF = 2.5) generated the highest reduction in sugar yield from grass silage. However, more severe reaction conditions of 180 °C for 20 min (SF = 3.7) favoured the degradation of sugars into inhibitory products such as HMF and furfural. The SFs of HTC reactions conducted in this study were 3.3 (150 °C), 4.7 (200 °C) and 6.2 (250 °C). Therefore, the hydrothermal pre-treatment conditions used in this study were too severe to result in enhanced biomethane generation. This is further supported by Wang et al. [33], who found a hydrothermal reaction severity of 4.4 (210 °C, 15 min) reduced biomethane yields by 33%

compared to untreated rice straw, likely due to the presence of fermentative inhibitors. However, reduced SF (0.9–3.5) had little effect on biomethane yields [33]. Again, this effect appears feedstock-dependent, as the HTC slurries produced from water hyacinth at 150 °C (SF = 3.3), 200 °C (SF = 4.7) and 250 °C (SF = 6.2) improved [E]BMP yields by 96%, 57%, and 42%, respectively, compared to raw water hyacinth [26]. However, raw water hyacinth had a lower BI (30%) and [E]BMP (103.1 mL CH_4/g VS) [26] compared to grass (Table 6), suggesting hydrothermal pre-treatment may be more suitable for feedstocks with lower biodegradabilities.

3.4. Energy Balance

The energy output of each HTC-AD integration option is shown in Figure 6 and compared to the energy output obtained from the AD of untreated grass: 8.76 MJ/kg. Figure 6a displays the energy output values obtained during the separation of HCs for combustion and PWs for biomethane generation by AD. Each HTC-AD integration strategy shown in Figure 6a resulted in an improvement in energy output compared to the AD of untreated grass. However, despite an improvement in ECE from 51% (grass) to 97% (150 °C), 83% (200 °C) and 68% (250 °C), ECE was reduced at higher processing temperatures. Literature studies [25–28,30] generally report a reduction in the energy output obtained from HC combustion and PW digestion as HTC temperature increases. HC combustion represented a greater energy output contribution compared to PW digestion and accounted for 82% (HTC-150), 85% (HTC-200) and 81% (HTC-250) of the total energy output. Similarly, water hyacinth-derived HCs contributed approximately 85% of the energy input using this integrated HTC-AD approach [26]. The energy output associated with HC combustion in Figure 6a reduced as HTC temperature increased, which was linked to a reduced HY and overall reduction in EY (Figure 1). The energy output associated with PW digestion was also greater for HTC-150 (2.93 MJ/kg) compared to HTC-200 or HTC-250 (2.14–2.15 MJ/kg), which was linked to a higher [E]BMP yield (Figure 5a) and COD concentration (Table 5).

Figure 6b indicates that HC digestion is not a suitable HTC-AD integration strategy, as the AD of HCs showed reduced ECE compared to the AD of untreated grass alone. HC combustion provides greater energy valorisation compared to HC digestion. Furthermore, Figure 6c shows HTC slurry digestion also reduced the ECE compared to the AD of untreated grass, suggesting hydrothermal pre-treatment using these conditions is not a suitable energy valorisation strategy for grass. Overall, separating HCs for combustion and PWs for AD was the HTC-AD integration strategy that yielded the greatest improvement in energy output compared to the AD of grass. This supports the conclusions of previous studies, which identified that the combustion of HCs and AD of PWs provided a greater energy output compared to the AD of HTC slurries for a range of feedstocks, including sewage sludge [30], macroalgae [25], water hyacinth [26] and the organic fraction of municipal solid waste [29].

Table 7 shows the energy return on energy invested (EROI) was highest for combined HC combustion and PW AD compared to other HTC-AD integration strategies across corresponding temperatures. Furthermore, this HTC-AD integration strategy yielded an EROI value > 1 across each processing temperature, indicating that each was an energetically feasible process.

The EROI reduced with increasing HTC temperature: 150 °C (6.76), 200 °C (4.15) and 250 °C (2.63), suggesting more favourable energetics at lower processing temperatures. However, the application of this HTC-AD integration strategy appears to be a compromise between desirable HC characteristics and favourable energetics. The results presented in Tables 2–4 and Figures 3 and 4 indicate that HC-250 possessed more desirable properties as a solid combustion fuel compared to HC-150 or HC-200, as it showed the greatest FC:VM, HHV, and ED and the highest removal of problematic inorganics, resulting in the greatest reduction in slagging and fouling. By comparison, HC-150 demonstrated limited ED (Figure 1) and more limited removal of problematic inorganics (Table 3). Therefore, the quality of HC as a combustion fuel appears compromised with less favourable energetics.
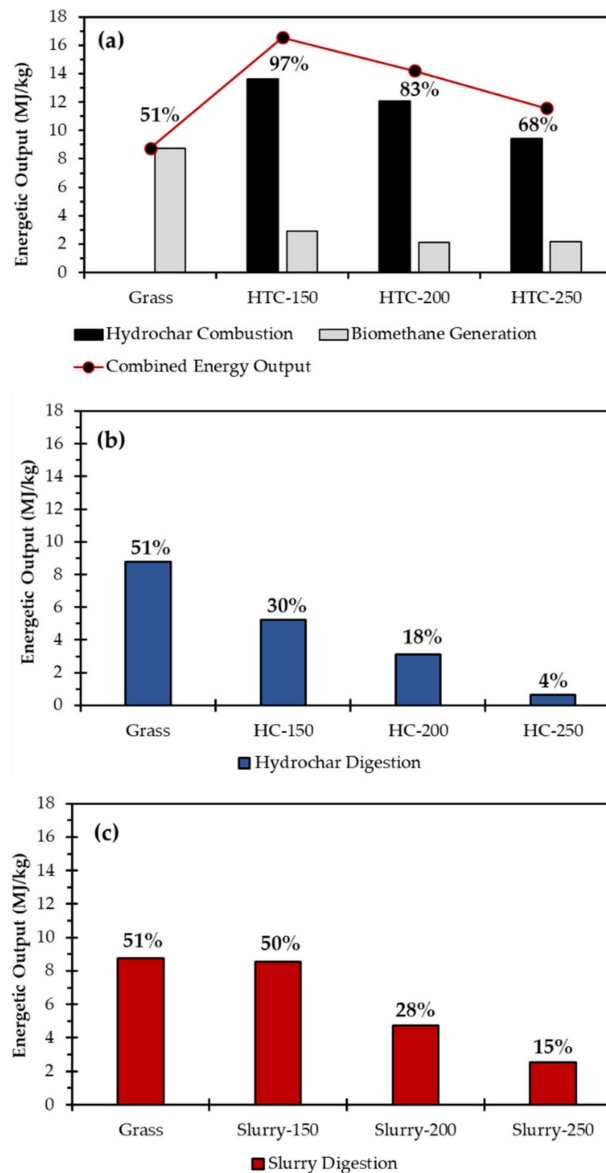
Figure 6. Energetic output of HTC-AD integration strategies: (**a**) combustion of hydrochar and digestion of process waters, (**b**) digestion of hydrochars only, and (**c**) digestion of HTC slurries, all based on 1 kg of oven dried grass. Percentages above the bars represent the energy conversion efficiency (ECE) of each integration strategy.

Table 7. Energy balance for HTC-AD integration strategies based on 1 kg oven dried grass.

HTC-AD Integration Strategy	Temperature (°C)	Energy Input (MJ/kg Grass)	Energy Output (MJ/kg Grass)	EROI *
Combined HC combustion and PW digestion	150	5.44	16.55	6.76
	200	7.61	14.21	4.15
	250	9.79	11.58	2.63
HC digestion alone	150	5.44	5.22	2.13
	200	7.61	3.10	0.91
	250	9.79	0.65	0.15
Slurry digestion	150	5.44	8.55	3.49
	200	7.61	4.75	1.39
	250	9.79	2.54	0.58

* Assumed 55% energy recovery efficiency [26]. EROI = energy return on energy invested.

4. Conclusions

The integration of hydrothermal carbonisation and anaerobic digestion (HTC-AD) can improve the energy conversion efficiency (ECE) of grass compared to anaerobic digestion (AD) alone. Separating hydrochars for combustion and process waters for digestion appears the most energetically feasible HTC-AD integration strategy, although lower hydrothermal carbonisation (HTC) processing temperatures resulted in more favourable energetics. Hydrochars represent the greater energy carrier compared to process waters. However, higher HTC temperatures produced hydrochars with more desirable combustion characteristics. The hydrochar produced at the highest temperature (250 °C) displayed the highest heating value (25.8 MJ/kg) and fixed carbon:volatile matter ratio (0.47) and the greatest reduction in slagging and fouling potential (ash flow temperature > 1550 °C). Integrating HTC-AD of grass at 250 °C improved ECE from 51% to 68% and appears to be an energy positive process (EROI = 2.63). However, more detailed analysis of the NO_x emissions from grass-derived hydrochars is required to facilitate the scaling up of this integrated technology.

Institutional Review Board Statement: Not applicable.

Informed Consent Statement: Not applicable.

Data Availability Statement: Data supporting this study are openly available under a CC-BY license at https://doi.org/10.5518/1154 (accessed on 13 March 2022).

Conflicts of Interest: The authors declare no conflict of interest.

References

1. Prochnow, A.; Heiermann, M.; Plöchl, M.; Linke, B.; Idler, C.; Amon, T.; Hobbs, P.J. Bioenergy from permanent grassland—A review: 1. Biogas. *Bioresour. Technol.* **2009**, *100*, 4931–4944. [CrossRef] [PubMed]
2. Smith, A.M.; Whittaker, C.; Shield, I.; Ross, A.B. The potential for production of high quality bio-coal from early harvested Miscanthus by hydrothermal carbonisation. *Fuel* **2018**, *220*, 546–557. [CrossRef]
3. Brown, A.E.; Ford, J.S.; Bale, C.S.E.; Camargo-Valero, M.A.; Cheffins, N.J.; Mason, P.E.; Price-Allison, A.M.; Ross, A.B.; Taylor, P.G. An assessment of road-verge grass as a feedstock for farm-fed anaerobic digestion plants. *Biomass Bioenergy* **2020**, *138*, 105570. [CrossRef]
4. Watson, L. The grass family, Poaceae. In *Reproductive Versatility in the Grasses*; Chapman, G.P., Ed.; Cambridge University Press: Cambridge, UK, 1990.
5. Wall, D.M.; O'Kiely, P.; Murphy, J.D. The potential for biomethane from grass and slurry to satisfy renewable energy targets. *Bioresour. Technol.* **2013**, *149*, 425–431. [CrossRef] [PubMed]
6. Rodriguez, C.; Alaswad, A.; Benyounis, K.Y.; Olabi, A.G. Pretreatment techniques used in biogas production from grass. *Renew. Sustain. Energy Rev.* **2017**, *68*, 1193–1204. [CrossRef]
7. Basu, P. *Biomass Gasification, Pyrolysis and Torrefaction: Practical Design and Theory*; Academic Press: Cambridge, MA, USA, 2013.
8. Smith, A.M.; Singh, S.; Ross, A.B. Fate of inorganic material during hydrothermal carbonisation of biomass: Influence of feedstock on combustion behaviour of hydrochar. *Fuel* **2016**, *169*, 135–145. [CrossRef]

9. Nitsche, M.; Hensgen, F.; Wachendorf, M. Using grass cuttings from sports fields for anaerobic digestion and combustion. *Energies* **2017**, *10*, 388. [CrossRef]

10. Smith, A.M.; Ross, A.B. The influence of residence time during hydrothermal carbonisation of miscanthus on bio-coal combustion chemistry. *Energies* **2019**, *12*, 523. [CrossRef]

11. Mihajlović, M.; Petrović, J.; Maletić, S.; Isakovski, M.K.; Stojanović, M.; Lopičić, Z.; Trifunović, S. Hydrothermal carbonization of Miscanthus × giganteus: Structural and fuel properties of hydrochars and organic profile with the ecotoxicological assessment of the liquid phase. *Energy Convers. Manag.* **2018**, *159*, 254–263. [CrossRef]

12. Reza, M.T.; Lynam, J.G.; Uddin, M.H.; Coronella, C.J. Hydrothermal carbonization: Fate of inorganics. *Biomass Bioenergy* **2013**, *49*, 86–94. [CrossRef]

13. Chiumenti, A.; Boscaro, D.; Da Borso, F.; Sartori, L.; Pezzuolo, A. Biogas from fresh spring and summer grass: Effect of the harvesting period. *Energies* **2018**, *11*, 1466. [CrossRef]

14. Cadavid Rodríguez, L.S.; Bolaños Valencia, I.V. Grass from public green spaces an alternative source of renewable energy in tropical countries. *Rev. Investig. Optim. Nuevos Procesos En Ing.* **2016**, *29*, 109–116. [CrossRef]

15. Wang, Y.; Li, Y.; Zhang, Y.; Song, Y.; Yan, B.; Wu, W.; Zhong, L.; Li, N.; Chen, G.; Hou, L. Hydrothermal carbonization of garden waste by pretreatment with anaerobic digestion to improve hydrohcar performance and energy recovery. *Sci. Total Environ.* **2022**, *807*, 151014. [CrossRef]

16. Yu, L.; Bule, M.; Ma, J.; Zhao, Q.; Frear, C.; Chen, S. Enhancing volatile fatty acid (VFA) and bio-methane production from lawn grass with pretreatment. *Bioresour. Technol.* **2014**, *162*, 243–249. [CrossRef]

17. UKERC Energy Data Centre. Phyllis2: Database for Biomass and Waste. Available online: https://phyllis.nl/Browse/Standard/ECN-Phyllis#grass (accessed on 3 March 2022).

18. Kruse, A.; Funke, A.; Titirici, M.M. Hydrothermal conversion of biomass to fuels and energetic materials. *Curr. Opin. Chem. Biol.* **2013**, *17*, 515–521. [CrossRef]

19. Kambo, H.S.; Dutta, A. A comparative review of biochar and hydrochar in terms of production, physico-chemical properties and applications. *Renew. Sustain. Energy Rev.* **2015**, *45*, 359–378. [CrossRef]

20. Funke, A.; Ziegler, F. Hydrothermal carbonization of biomass: A summary and discussion of chemical mechanisms for process engineering. *Biofuels Bioprod. Biorefining* **2010**, *4*, 160–177. [CrossRef]

21. Qadi, N.; Takeno, K.; Mosqueda, A.; Kobayashi, M.; Motoyama, Y.; Yoshikawa, K. Effect of Hydrothermal Carbonization Conditions on the Physicochemical Properties and Gasification Reactivity of Energy Grass. *Energy Fuels* **2019**, *33*, 6436–6443. [CrossRef]

22. Guo, S.; Dong, X.; Liu, K.; Yu, H.; Zhu, C. Chemical, energetic, and structural characteristics of hydrothermal carbonization solid products for lawn grass. *BioResources* **2015**, *10*, 4613–4625. [CrossRef]

23. Ipiales, R.P.; de la Rubia, M.A.; Diaz, E.; Mohedano, A.F.; Rodriguez, J.J. Integration of Hydrothermal Carbonization and Anaerobic Digestion for Energy Recovery of Biomass Waste: An Overview. *Energy Fuels* **2021**, *35*, 17032–17050. [CrossRef]

24. Becker, R.; Dorgerloh, U.; Paulke, E.; Mumme, J.; Nehls, I. Hydrothermal carbonization of biomass: Major organic components of the aqueous phase. *Chem. Eng. Technol.* **2014**, *37*, 511–518. [CrossRef]

25. Brown, A.E.; Finnerty, G.L.; Camargo-Valero, M.A.; Ross, A.B. Valorisation of Macroalgae via the Integration of Hydrothermal Carbonisation and Anaerobic Digestion. *Bioresour. Technol.* **2020**, *312*, 123539. [CrossRef] [PubMed]

26. Brown, A.E.; Adams, J.M.M.; Grasham, O.R.; Camargo-valero, M.A.; Ross, A.B. An Assessment of Different Integration Strategies of Hydrothermal Carbonisation and Anaerobic Digestion of Water Hyacinth. *Energies* **2020**, *13*, 5983. [CrossRef]

27. Marin-Batista, J.D.; Villamil, J.A.; Rodriguez, J.J.; Mohedano, A.F.; Rubia, M.A. De Valorization of microalgal biomass by hydrothermal carbonization and anaerobic digestion. *Bioresour. Technol.* **2019**, *274*, 395–402. [CrossRef] [PubMed]

28. Marin-Batista, J.D.; Villamil, J.A.; Qaramaleki, S.V.; Coronella, C.J.; Mohedano, A.F.; de la Rubia, M.A. Energy valorization of cow manure by hydrothermal carbonization and anaerobic digestion. *Renew. Energy* **2020**, *160*, 623–632. [CrossRef]

29. Lucian, M.; Volpe, M.; Merzari, F.; Wüst, D.; Kruse, A.; Andreottola, G.; Fiori, L. Hydrothermal carbonization coupled with anaerobic digestion for the valorization of the organic fraction of municipal solid waste. *Bioresour. Technol.* **2020**, *314*, 123734. [CrossRef]

30. Aragón-Briceño, C.; Ross, A.B.; Camargo-Valero, M.A. Evaluation and comparison of product yields and bio-methane potential in sewage digestate following hydrothermal treatment. *Appl. Energy* **2017**, *208*, 1357–1369. [CrossRef]

31. Luz, F.C.; Volpe, M.; Fiori, L.; Manni, A.; Cordiner, S.; Mulone, V.; Rocco, V. Spent coffee enhanced biomethane potential via an integrated hydrothermal carbonization-anaerobic digestion process. *Bioresour. Technol.* **2018**, *256*, 102–109. [CrossRef]

32. Lin, R.; Deng, C.; Ding, L.; Bose, A.; Murphy, J.D. Improving gaseous biofuel production from seaweed Saccharina latissima: The effect of hydrothermal pretreatment on energy efficiency. *Energy Convers. Manag.* **2019**, *196*, 1385–1394. [CrossRef]

33. Wang, D.; Shen, F.; Yang, G.; Zhang, Y.; Deng, S.; Zhang, J.; Zeng, Y.; Luo, T.; Mei, Z. Can hydrothermal pretreatment improve anaerobic digestion for biogas from lignocellulosic biomass? *Bioresour. Technol.* **2018**, *249*, 117–124. [CrossRef]

34. Parmar, K.R.; Ross, A.B. Integration of Hydrothermal Carbonisation with Anaerobic Digestion; Opportunities for Valorisation of Digestate. *Energies* **2019**, *12*, 1586. [CrossRef]

35. Pagés-Díaz, J.; Alvarado, A.O.C.; Montalvo, S.; Diaz-Robles, L.; Curio, C.H. Anaerobic bio-methane potential of the liquors from hydrothermal carbonization of different lignocellulose biomasses. *Renew. Energy* **2020**, *157*, 182–189. [CrossRef]

36. Parmar, K.R.; Brown, A.E.; Hammerton, J.M.; Camargo-Valero, M.A.; Fletcher, L.A.; Ross, A.B. Co-Processing Lignocellulosic Biomass and Sewage Digestate by Hydrothermal Carbonisation: Influence of Blending on Product Quality. *Energies* **2022**, *15*, 1418. [CrossRef]

37. Heidari, M.; Norouzi, O.; Salaudeen, S.; Acharya, B.; Dutta, A. Prediction of Hydrothermal Carbonization with Respect to the Biomass Components and Severity Factor. *Energy Fuels* **2019**, *33*, 9916–9924. [CrossRef]

38. Raposo, F.; Fernández-Cegrí, V.; de la Rubia, M.A.; Borja, R.; Béline, F.; Cavinato, C.; Demirer, G.; Fernández, B.; Fernández-Polanco, M.; Frigon, J.C.; et al. Biochemical methane potential (BMP) of solid organic substrates: Evaluation of anaerobic biodegradability using data from an international interlaboratory study. *J. Chem. Technol. Biotechnol.* **2011**, *86*, 1088–1098. [CrossRef]

39. *APHA Standard Methods for the Examination of Water and Wastewater*; American Public Health Association: Washington, DC, USA, 2005.

40. He, C.; Giannis, A.; Wang, J.Y. Conversion of sewage sludge to clean solid fuel using hydrothermal carbonization: Hydrochar fuel characteristics and combustion behavior. *Appl. Energy* **2013**, *111*, 257–266. [CrossRef]

41. Mitchell, E.J.S.; Lea-Langton, A.R.; Jones, J.M.; Williams, A.; Layden, P.; Johnson, R. The impact of fuel properties on the emissions from the combustion of biomass and other solid fuels in a fixed bed domestic stove. *Fuel Process. Technol.* **2016**, *142*, 115–123. [CrossRef]

42. Andriamanohiarisoamanana, F.J.; Matsunami, N.; Yamashiro, T.; Iwasaki, M.; Ihara, I.; Umetsu, K. High-solids anaerobic mono-digestion of riverbank grass under thermophilic conditions. *J. Environ. Sci.* **2017**, *52*, 29–38. [CrossRef]

43. Munawer, M.E. Human health and environmental impacts of coal combustion and post-combustion wastes. *J. Sustain. Min.* **2018**, *17*, 87–96. [CrossRef]

44. Zhang, C.; Ma, X.; Chen, X.; Tian, Y.; Zhou, Y.; Lu, X.; Huang, T. Conversion of water hyacinth to value-added fuel via hydrothermal carbonization. *Energy* **2020**, *197*, 117193. [CrossRef]

45. Reza, M.T.; Andert, J.; Wirth, B.; Busch, D.; Pielert, J.; Lynam, J.G.; Mumme, J. Hydrothermal Carbonization of Biomass for Energy and Crop Production. *Appl. Bioenergy* **2014**, *1*, 11–29. [CrossRef]

46. Nizamuddin, S.; Baloch, H.A.; Griffin, G.J.; Mubarak, N.M.; Bhutto, A.W.; Abro, R.; Mazari, S.A.; Ali, B.S. An overview of effect of process parameters on hydrothermal carbonization of biomass. *Renew. Sustain. Energy Rev.* **2017**, *73*, 1289–1299. [CrossRef]

47. Smith, A.M. Fate and Influence of Inorganics and Heteroatoms during the Hydrothermal Carbonisation of Biomass. Ph.D. Thesis, University of Leeds, Leeds, UK, 2018.

48. Machado, N.T.; de Castro, D.A.R.; Santos, M.C.; Araújo, M.E.; Lüder, U.; Herklotz, L.; Werner, M.; Mumme, J.; Hoffmann, T. Process analysis of hydrothermal carbonization of corn Stover with subcritical H_2O. *J. Supercrit. Fluids* **2018**, *136*, 110–122. [CrossRef]

49. Nakason, K.; Panyapinyopol, B.; Kanokkantapong, V.; Viriya-empikul, N.; Kraithong, W.; Pavasant, P. Hydrothermal carbonization of unwanted biomass materials: Effect of process temperature and retention time on hydrochar and liquid fraction. *J. Energy Inst.* **2017**, *91*, 786–796. [CrossRef]

50. Yenigün, O.; Demirel, B. Ammonia inhibition in anaerobic digestion: A review. *Process Biochem.* **2013**, *48*, 901–911. [CrossRef]

51. Monlau, F.; Sambusiti, C.; Barakat, A.; Quéméneur, M.; Trably, E.; Steyer, J.P.; Carrère, H. Do furanic and phenolic compounds of lignocellulosic and algae biomass hydrolyzate inhibit anaerobic mixed cultures? A comprehensive review. *Biotechnol. Adv.* **2014**, *32*, 934–951. [CrossRef]

52. Deng, C.; Lin, R.; Cheng, J.; Murphy, J.D. Can acid pre-treatment enhance biohydrogen and biomethane production from grass silage in single-stage and two-stage fermentation processes ? *Energy Convers. Manag.* **2019**, *195*, 738–747. [CrossRef]

53. Nizami, A.S.; Orozco, A.; Groom, E.; Dieterich, B.; Murphy, J.D. How much gas can we get from grass? *Appl. Energy* **2012**, *92*, 783–790. [CrossRef]

54. Raju, C.S.; Ward, A.J.; Nielsen, L.; Møller, H.B. Comparison of near infra-red spectroscopy, neutral detergent fibre assay and in-vitro organic matter digestibility assay for rapid determination of the biochemical methane potential of meadow grasses. *Bioresour. Technol.* **2011**, *102*, 7835–7839. [CrossRef]

55. Zhang, Y.; Kusch-Brandt, S.; Salter, A.M.; Heaven, S. Estimating the methane potential of energy crops: An overview on types of data sources and their limitations. *Processes* **2021**, *9*, 1565. [CrossRef]

56. Erdogan, E.; Atila, B.; Mumme, J.; Reza, M.T.; Toptas, A.; Elibol, M.; Yanik, J. Characterization of products from hydrothermal carbonization of orange pomace including anaerobic digestibility of process liquor. *Bioresour. Technol.* **2015**, *196*, 35–42. [CrossRef]

57. Hoekman, S.K.; Broch, A.; Robbins, C. Hydrothermal carbonization (HTC) of lignocellulosic biomass. *Energy Fuels* **2012**, *25*, 1802–1810. [CrossRef]

58. Ward, A.J.; Hobbs, P.J.; Holliman, P.J.; Jones, D.L. Optimisation of the anaerobic digestion of agricultural resources. *Bioresour. Technol.* **2008**, *99*, 7928–7940. [CrossRef]

59. Mumme, J.; Srocke, F.; Heeg, K.; Werner, M. Use of biochars in anaerobic digestion. *Bioresour. Technol.* **2014**, *164*, 189–197. [CrossRef]

60. Lin, R.; Deng, C.; Rajendran, K.; Bose, A.; Kang, X.; Murphy, J.D. Competing Reactions Limit Production of Sugars in Hydrothermal Hydrolysis of Grass Silage: An Assessment of the Effect of Temperature on Sugar Production and Parasitic Energy Demand. *Front. Energy Res.* **2020**, *8*, 255. [CrossRef]